Naval Research Laboratory

Washington, DC 20375-5000

DTIC FILE COPY

AD-A186 212

Numerical Prediction of Thermal Ship Wakes

MICHAEL STEWART

Laboratory for Computational Physics and Fluid Dynamics
Center for Hydrodynamic Developments

September 4, 1987

DTIC
SELECTED
OCT 0 1 1987
D

'87 9 23 255

REPORT DOCUMENTATION PAGE

1a. REPORT SECURITY CLASSIFICATION UNCLASSIFIED		1b RESTRICTIVE MARKINGS			
2a. SECURITY CLASSIFICATION AUTHORITY		3 DISTRIBUTION/AVAILABILITY OF REPORT Approved for public release; distribution unlimited.			
2b. DECLASSIFICATION/DOWNGRADING SCHEDULE					
4. PERFORMING ORGANIZATION REPORT NUMBER(S) NRL Memorandum Report 5955		5. MONITORING ORGANIZATION REPORT NUMBER(S)			
6a. NAME OF PERFORMING ORGANIZATION Naval Research Laboratory	6b. OFFICE SYMBOL (If applicable)	7a. NAME OF MONITORING ORGANIZATION			
6c. ADDRESS (City, State, and ZIP Code) Washington, DC 20375-5000		7b. ADDRESS (City, State, and ZIP Code)			
8a. NAME OF FUNDING/SPONSORING ORGANIZATION	8b. OFFICE SYMBOL (If applicable)	9. PROCUREMENT INSTRUMENT IDENTIFICATION NUMBER			
8c. ADDRESS (City, State, and ZIP Code)		10. SOURCE OF FUNDING NUMBERS			
		PROGRAM ELEMENT NO.	PROJECT NO.	TASK NO	WORK UNIT ACCESSION NO.

11. TITLE (Include Security Classification)
Numerical Prediction of Thermal Ship Wakes

12. PERSONAL AUTHOR(S)
Stewart, M.

13a. TYPE OF REPORT	13b. TIME COVERED FROM____ TO____	14. DATE OF REPORT (Year, Month, Day) 1987 September 4	15. PAGE COUNT 30

16. SUPPLEMENTARY NOTATION

17.	COSATI CODES		18. SUBJECT TERMS (Continue on reverse if necessary and identify by block number)
FIELD	GROUP	SUB-GROUP	Thermal ship wake Numerical fluid dynamics
			Finite volume Hydrodynamics

19. ABSTRACT (Continue on reverse if necessary and identify by block number)

A numerical model of the thermal wake caused by turbulent water motion directly behind a ship is described. The model is a finite volume formulation of the parabolic Navier-Stokes equations. The effects of turbulence are modeled using the turbulent kinetic energy/dissipation equations with an anisotropic Reynolds stress closure. This procedure gives reasonable agreement with David Taylor NSRDC model data for the momentum wake. The energy equations are solved subject to boundary conditions consistent with radiative, convective, latent heat transfer at the ocean surface and a volumetric solar source term which decays exponentially with depth. The effect of wind stress on the thermal wake is included approximately. The coupling from the energy equation to the momentum equations employs the Boussinesq approximation. This procedure, when used in free shear flows, appears to give a qualitative representation of the effect of buoyancy. Numerical experiments were performed to determine the effect of other factors in the growth and decay of the thermal wakes of surface ships.

20. DISTRIBUTION/AVAILABILITY OF ABSTRACT ☒ UNCLASSIFIED/UNLIMITED ☐ SAME AS RPT. ☐ DTIC USERS	21. ABSTRACT SECURITY CLASSIFICATION UNCLASSIFIED	
22a. NAME OF RESPONSIBLE INDIVIDUAL Michael Stewart	22b. TELEPHONE (Include Area Code) (202) 767-2904	22c. OFFICE SYMBOL Code 4430

DD FORM 1473, 84 MAR   83 APR edition may be used until exhausted.
All other editions are obsolete

☆U.S. Government Printing Office: 1985—807-047

CONTENTS

NUMERICAL PREDICTION OF THERMAL WAKES

Introduction

Wake detection has long been considered as a valuable tool for the location and identification of ships, i.e. (1). The white water wake was first used for this purpose (2) by aerial observation during the second world war. Later, attempts were made to determine if the thermal disturbance could be detected by bow mounted thermistors on submarines to locate surface ships (1). More recently active and passive electromagnetic remote sensors have been used to detect the various elements of ship wakes (3).

Background

Ships moving through the ocean will produce disturbances in and around the wake which can be detected using a variety of remote sensors. A thorough understanding of the causes and the evolution of these wake disturbances can, in principle, provide information about the type of ship, its speed and course, and probably the ambient weather conditions.

The first major ship-generated disturbance is an inviscid Kelvin wake which radiates away from the ship. This wake can be detected either visually or with radar. It has been modeled for a variety of ships and ambient sea conditions (4).

The second major type of disturbance is the turbulent wake confined to a narrow region behind the ship. Imbedded in the turbulent wake are vortices created by the bow wave, the bilges and the propeller. This wake has been the subject of considerable study using a variety of techniques including inviscid vortex procedures, linearized Navier-Stokes solvers, and more recently, a parabolic Navier-Stokes solver with a k/epsilon turbulence model. A review is found in (5).

A third disturbance is the white water wake caused by entrained air formed by the bow wave and inside the turbulent wake by the bilges and the propeller. The phenomena of air entrainment have not been modeled although the evolution of a bubble wake has been modeled under simplified situations by tracking individual bubbles (6) or by using the equations governing bubble dynamics (7).

Another type of wake feature is the thermal "scar" formed by the fluid motion inside the turbulent wake and, to a lesser extent, changes in the radiative properties of the free surface as the ship induced current interacts with the ambient wave field and wind. There has been little or no work done to model this wake which is remotely sensible by passive radiometric techniques in the infrared (IR) and microwave (MR) bands.

Observations of this wake show two distinct parts of the thermal wake. The subsurface wake (1) is fairly predictable and remarkably persistent, often lasting 60 minutes. The surface scar (3) appears to be more variable and is less persistent, typically disappearing after about 20 minutes.

1

A more complete understanding of the dynamics of turbulent thermal wakes is needed as an element of a detectability assessment for surface ship wakes. The processes by which thermal wakes are formed, how they decay, and the effect of ambient wind, temperature, and sun are not well known. This report contains a model of the establishment of the thermal wake and evaluations of the factors which influence its development.

Thermal Structure of the Open Ocean

The variation in ocean temperature is influenced by many factors. Even without the presence of external disturbances, such as ships, the ocean temperature is rarely uniform. Typically, the variation of temperature with depth is divided into several regions. The upper-most region is a surface micro layer found at the interface between the ocean and the atmosphere. This layer is typically less than 1 mm thick and is characterized by the dominance of molecular interactions over turbulent or convective interactions. At this laminar layer, heat lost to the atmosphere through long wave radiation to the sky, convection to the air, and latent heat loss through evaporation is balanced by conduction to the turbulent mixed layer below.

This layer is also associated with large influences of surface-active, monolayers of organic films (8). The role of these films in oceanographic and wake processes is not well known and is becoming a subject of some concern. Film effects are not included in this study.

Below the surface micro layer is the 'mixed layer' which is dominated by turbulent and convective transport properties and is considered to be uniform in temperature. This is caused by the relatively vigorous mixing due to wind and wave motion at the ocean surface, called thermocline erosion, and the fact that the large majority of solar radiation is absorbed in this layer. Below this layer is a thermocline after which the water temperature gradually cools until, at very deep locations, the water temperature approaches freezing. The mixed layer usually extends from 20 to 50 meters below the surface and will be the deepest region of interest in this study.

In addition to variations with depth, the ocean temperature also varies in the horizontal direction due to the presence of oceanic fronts and currents. As a ship passes through a front, the characteristics of the thermal wake can change dramatically (3).

If the mixed layer was completely uniform in temperature there would be no observable thermal wake. The bulk mixing due to the passage of a ship would cause no change in water temperature. There are two situations where an appreciable vertical temperature gradient can exist in the upper mixed layer.

The first situation occurs when wind and wave mixing is weak. Thermocline erosion can decrease to such an extent that solar heating, which decays exponentially with depth, causes an exponential temperature decay with water depth. This temperature variation can be substantial but due to the extended depth of the profile and the large heat capacity of water it usually only occurs during the afternoon of relatively quiet, cloudless days. During the day solar heating effects dominate the infrared signature of the ambient ocean. The mixed layer can increase in temperature by several degrees Celsius and reflected and scattered solar radiation mask emissions by the surface microlayer.

The second situation occurs at night. Turbulent and convective mixing eliminate temperature variations in the mixed layer. Long wave thermal radiation produces a temperature gradient of .1-.2 C in the surface microlayer where thermal conduction dominates. The absence of solar radiation and temperature variations in the subsurface mixed layer allows this temperature profile across the surface microlayer to become easily visible in the infrared spectrum.

2

Procedure

As mentioned previously, a reasonable model of the turbulent wake behind a ship currently exists (9). The same basic approach was used to model the thermal disturbance behind a ship. Instead of the finite element code which has been used for predicting the turbulent wake, a finite volume code was chosen for ease of code development. The same form of the Navier-Stokes equations and the Reynolds stress closure was employed here. The parabolic form of the Navier-Stokes equations, the energy equation, the turbulent kinetic energy and dissipation, and the Reynolds stress closure are shown in Table 1.

This form of the parabolic Navier-Stokes equations have been derived in (10). They are formed using the usual boundary layer ordering of terms which eliminates the axial diffusion of momentum and heat. When coupled with the one-way axial flow and the assumption of small streamline curvature, the elliptical nature of the equations is retained only in the transverse directions.

Integration of these equations begins with the initial velocity and temperature field behind the ship. All equations are marched downstream using time (or if you wish, spatial) steps small enough to eliminate the need for iteration. After each time step, the elliptic boundary conditions are satisfied for the velocity and temperature fields only in the transverse direction. The continuity equation is satisfied by adjusting the transverse pressure distribution using a Poisson equation. The axial pressure distribution is assumed to be the same as in the far fluid, in this case zero gradient.

The procedure can be modified when the effects of streamline curvature become significant. The three dimensional pressure field is calculated and stored during each sweep through the calculation region and several iterations of the entire calculation are required. The advantage of this type of 'partially parabolic' scheme over a fully elliptic version is only in computer storage as only the pressure is stored in three dimensions. Execution time is roughly the same as an elliptical procedure. In the case of ship wakes, it may be possible to divide the computations into a partially parabolic region near the ship stern and a fully parabolic region extending downstream from a point after the swirl velocities become sufficiently small. This would retain most of the computational efficiency of a parabolic scheme while improving the high swirl predictions only where they are needed.

The energy equation is slightly simplified when compared to the momentum equations. The form of the energy equation suggested in (11) uses velocity-stagnation enthalphy correlations to model the turbulent transport of heat. No models of these correlations were proposed. Although non-isotropic versions of these correlations can be found elsewhere, i.e. (12), it is unlikely that they would be significantly more accurate than isotropic versions considering the different modeling assumptions used. Therefore, isotropic fluctuating velocity-temperature correlations were included in the present calculations.

The boundary conditions for the temperature field are the usual ones (9) except at the free surface. There, heat is added or removed by infrared radiation between the water and the sky (or clouds), convective heat transfer between the water and air, and latent heat transfer proportional to the evaporation rate. All three effects are confined to the surface microlayer of the water. These effects are modeled using correlations available from the literature (13). Convective sensible/latent heat transfer is proportional to the wind speed times the temperature/vapor pressure difference between the sea surface and the air 10 m above. Long wave thermal radiation is constant.

The solar flux responsible for the vertical temperature in the gradient is absorbed over a much larger region of the ocean. Depending on the turbidity of the water, solar heating is usually restricted to the top 10 meters. A two dimensional simulation of the ocean surface was made to assess the time constant characteristic of solar heating and provide initial conditions for the ship wake. The transient temperature profiles shown in Fig. 1 indicates that several hours are needed to influence the ocean temperature significantly. This transient lasts much longer than the thermal wake is expected to be

3

Table 1 — Parabolic Navier-Stokes Equations, Energy
Equation and Reynolds Stress

$$\frac{\partial}{\partial x}(\rho u^2) + \frac{\partial}{\partial y}(\rho v u) + \frac{\partial}{\partial z}(\rho \omega u) = \frac{\partial \tau'_{u,xz}}{\partial y} + \frac{\partial \tau'_{u,xy}}{\partial z} - \frac{\partial \bar{P}}{\partial x} + Fu$$

$$\frac{\partial}{\partial x}(\rho u v) + \frac{\partial}{\partial y}(\rho v^2) + \frac{\partial}{\partial z}(\rho \omega v) = \frac{\partial \tau'_{v,xz}}{\partial y} + \frac{\partial \tau'_{v,xy}}{\partial z} - \frac{\partial P}{\partial y} + F v$$

$$\frac{\partial}{\partial x}(\rho u \omega) + \frac{\partial}{\partial y}(\rho v \omega) + \frac{\partial}{\partial z}(\rho \omega^2) = \frac{\partial \tau'_{\omega,xz}}{\partial y} + \frac{\partial \tau'_{\omega,xy}}{\partial z} - \frac{\partial P}{\partial z} + F\omega$$

$$\frac{\partial}{\partial x}(\rho u \phi) + \frac{\partial}{\partial y}(\rho v \phi) + \frac{\partial}{\partial z}(\rho \omega \phi) = -\frac{\partial}{\partial y}(J'_{\phi,xz} - \frac{\partial}{\partial z}(J'_{\phi,xy}) + S\phi$$

$$\frac{\partial}{\partial x}(\rho u) + \frac{\partial}{\partial y}(\rho v) + \frac{\partial}{\partial z}(\rho \omega) = 0$$

where

τ' is the total Reynolds and molecular stress

$\frac{\partial p}{\partial x}$ is known prior to the calculation

$P(y,z)$ is adjusted to satisfy conti roman vity

$\phi = T, k, \epsilon$ — any fluid property which can be convected and diffused

J' is the total turbulent and molecular diffusion

u, x act in the streamwise coordinate direction

v, y act in the horizontal, transverse coordinate direction

ω, z act in the vertical, transverse coordinate direction

F are momentum source terms e.g. buoyancy, wind stress

S are the property source terms, solar heating, turbulent production/dissipation

Reynolds Stresses

$$\overline{u'^2} = C_1 k - C_2 C_4 \frac{K'}{\epsilon^2} \left[\left(\frac{\partial u}{\partial y} \right)^2 + \left(\frac{\partial u}{\partial z} \right)^2 \right] - 2 c_4 \frac{k_2}{\epsilon} \left(\frac{\partial u}{\partial x} \right)$$

4

$$\overline{v'^2} = C_3 k - C_2 C_4 \frac{K^3}{\epsilon} \left[\left(\frac{\partial u}{\partial y} \right)^2 \right] - 2 C_4 \frac{K^2}{\epsilon} \frac{\partial v}{\partial y}$$

$$\overline{\omega'^2} = C_3 k - C_2 C_4 \frac{k^3}{\epsilon} \left[\left(\frac{\partial u}{\partial z} \right)^2 \right] - 2 C_4 \frac{k^2}{\epsilon} \frac{\partial \omega}{\partial z}$$

$$\overline{u'v'} z - C_4 \frac{k^2}{\epsilon} \frac{\partial u}{\partial y} - C_2 C_4 \frac{K^3}{\epsilon^2} \left[\frac{\partial u}{\partial z} \left(\frac{\partial v}{\partial z} + \frac{\partial w}{\partial y} \right) + 2 \frac{\partial u}{\partial y} \left(\frac{\partial u}{\partial x} + \frac{\partial v}{\partial y} \right) \right]$$

$$\overline{u'\omega'} = - C_4 \frac{k^2}{\epsilon} \frac{\partial u}{\partial z} - C_2 C_4 \frac{k^3}{\epsilon^2} \left[\frac{\partial u}{\partial y} \left(\frac{\partial \omega}{\partial y} + \frac{\partial v}{\partial z} \right) + 2 \frac{\partial u}{\partial z} \left(\frac{\partial u}{\partial x} + \frac{\partial \omega}{\partial z} \right) \right]$$

$$v' \omega' = - {}_2 C_4 \frac{K^2}{\epsilon^2} \left[\frac{\partial u}{\partial y} \frac{\partial u}{\partial z} \right] - C_4 \frac{K^2}{\epsilon} \left(\frac{\partial v}{\partial z} + \frac{\partial \omega}{\partial y} \right)$$

Turbulent Heat Flux

$$\overline{u't'} = \sigma_T C_4 \frac{k^2}{\epsilon} \frac{\partial T}{\partial x}$$

$$\overline{v't'} = \sigma_T C^4 \frac{K^2}{\epsilon} \frac{\partial T}{\partial y}$$

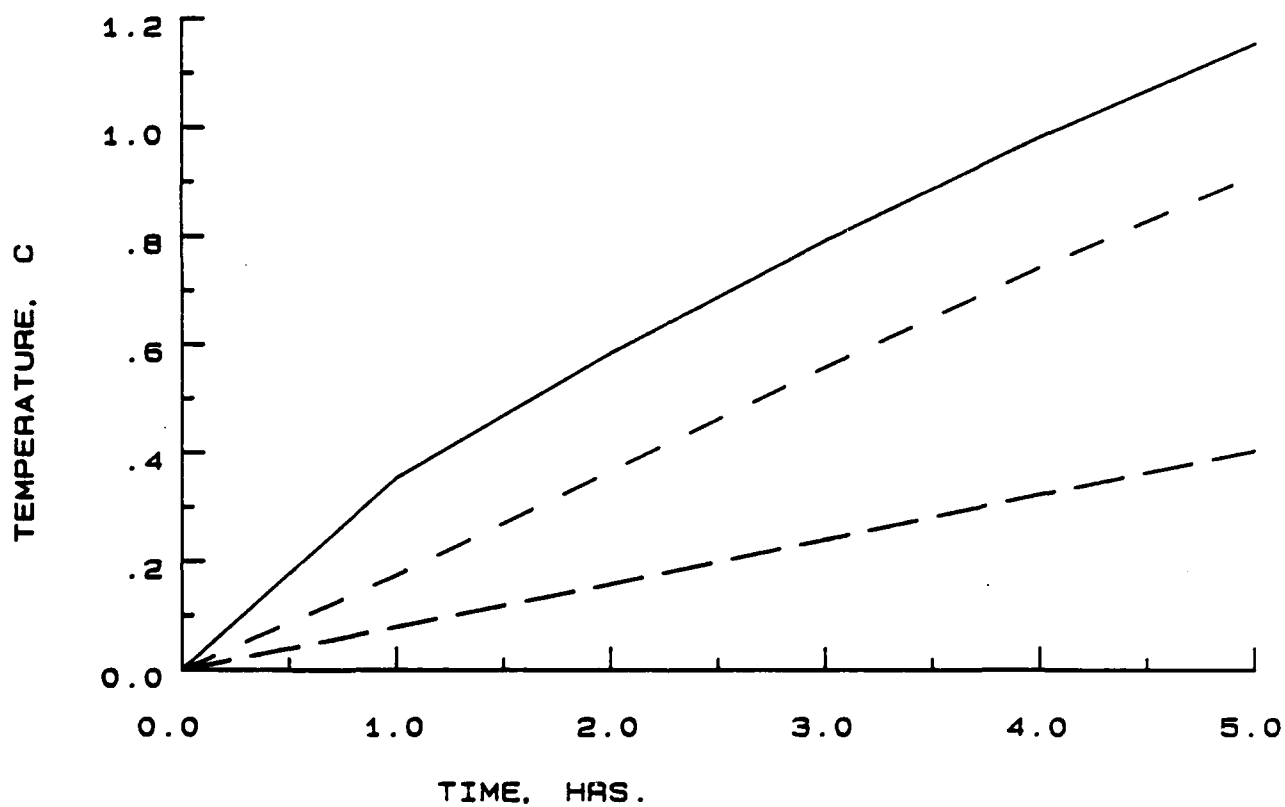$$\overline{\omega'T'} = \sigma_T c_4 \frac{k^2}{\epsilon} \frac{\partial T}{\partial z}$$

Fig. 1 — Ambient Ocean Temperature Profile Development

6

detectable (1,3). Therefore, although the solar influences will be retained as source terms, their effect on the calculated thermal wake will be small.

Additional features have been added to the energy equation to in the course of numerical experiments to evaluate the effect of gross anisotropy of the thermal diffusivity, wind stress, buoyancy, and the nighttime cold layer. These modifications will be described later in the report.

Verification of the code was made using ship model test data supplied from David Taylor NSRDC. Comparisons were made of the axial and swirl velocity components and two of the normal Reynolds stresses. The agreement was reasonable. No temperature measurements were available.

A benefit arising from using a special purpose finite volume code was much more efficient storage and execution time. Initially, the Cray XMP supercomputer was to be used for this study based on earlier runs made with the finite element code on a PDP Vax 780. The control volume code ran 10 to 20 times faster than the finite element code. Based on these results, the code could be easily used on a minicomputer.

Results and Discussion

The initial velocity conditions used for this series of thermal wake simulations were provided from estimates of the turbulent wake produced by the Kaimalino, a small waterplane area/twin hull (SWATH) ship operated by the U.S. Navy. This wake is slightly simpler than conventional ship wakes. The largest part of the hull is an axisymmetric body which is completely submerged. This is connected to the superstructure by a relatively thin strut. A horizontal stabilizer connecting the hulls and a forward canard complete the underwater structure.

In this type of hull, the dominant wake structure is the propeller vortex and jet (thrust) superimposed on the drag wake of the axisymmetric body. This wake is initially completely submerged and only interacts with the free surface some distance behind the ship. Small necklace vortices will be formed at the joints between the strut and control surfaces and the body. A weak drag wake and Kelvin wake will be formed by the strut and control surfaces. Due to limitations of the empirical scheme used to predict the initial conditions, the necklace vortices and Kelvin wake were ignored. The turbulent wakes from the strut, stabilizer, and canard were included.

A conventional ship hull has a much more complex shape producing strong vortices from the bilges which interact with the propeller vortices to produce a multiple vortex pattern behing the ship which is difficult to predict using empirical methods. In addition, the Kelvin wake is much stronger and transient ship motion (roll and pitch) can also produce strong wake components. Moreover, all parts of a conventional ship wake are formed near to the free surface which means that not only are the various components interacting with each other at the onset, they are also likely to all be influenced by free surface conditions and processes.

Thus, using the SWATH wake, the characteristics of the thermal wake can be more easily traced to particular structures of the turbulent wake. In addition, the interaction of the hull with the free surface is less than that of a conventional hull. The effects of the interactions between the free surface and turbulence are reduced as well as any effect of the Kelvin wave pattern.

The initial velocity, turbulent kinetic energy, and turbulent dissipation profiles were estimated by superimposing empirical correlations for the flow past simple geometric bodies to approximate the underwater portion of the Kaimalino hull. The initial temperature distribution in the upper ocean was calculated using a two dimensional control volume model. This model assumes constant turbulence

7

parameters, incident solar flux, and surface heat transfer. Solar radiation absorption as a function of depth was calculated using low turbidity water (14). The model was run for 5 hours of solar heating which produced approximately a 1 degree temperature difference between the water surface and the layer 10 meters deep. This profile was fitted with an exponential equation and then used as initial conditions in the model. The initial isotherms and swirl velocity distribution are shown in Figs. 2a and 2b.

Initial Wake Development

Using these initial conditions, the solar source term, and the surface heat flux, the thermal wake was calculated starting behind the ship and extending 3 km downstream. The results of this calculation are shown in Figs. 3a and 3b. The surface thermal wake begins some distance behind the ship when the propeller vortex rises (or expands) enough to reach the surface. Even 3 km behind the ship, the surface wake is growing in intensity. Although not shown here, this behavior continues far beyond the 3 km station.

The effect of the propeller vortex on the isotherms is shown in Fig. 3b. The swirl velocity wraps the isotherms into a spiral and the effect of turbulent diffusivity is enough that some diffusion of the temperature gradients is seen. This behavior was observed qualitatively in (1).

Infrared observations of the thermal wakes of ships (3) show the wake disappearing within 3 to 5 km. In situ measurements (1) have detected subsurface wakes at 3 to 4 times this distance. It appears from the numerical calculations that the subsurface wake persists because the primary mechanism of heat transport is convective. This is consistent with the low wind speeds necessary for the development of a temperature profile which causes low ambient turbulence intensities in the water. In the absence of the effects of a strong density stratification, the propeller vortex which pumps the cold water to the surface is essentially inviscid and decays very slowly. The surface scar, however, appears to have another mechanism which interferes with the development and eventually causes the surface scar to heal.

Surface Scar Healing

Several mechanisms which might account for the eventual healing of the thermal surface scar were identified. A numerical scheme was developed for each to evaluate its potential. The results of each are discussed with the available experimental observations in the following paragraphs.

From the initial results, it appears that the effective thermal diffusivity has a small role in the development of the wake. This effective diffusivity is modeled using the turbulent kinetic energy and dissipation calculated as part of the Reynolds stress model. There is also assumed to be a minimum background diffusivity in the ocean (15). Two numerical experiments were performed to estimate the sensitivity of the calculations to 1) the background turbulence level and 2) the anisotropy which may be caused by shear layers i.e., wind or current. The interactions between the free surface and turbulent anisotropy were not modelled here.

The first experiment involved simply increasing the minimum value of the thermal diffusivity by an order of magnitude. The results, shown in Figs. 4a and 4b show the isotherms becoming slightly diffused over a larger area. Despite the larger internal heat transfer, the scar does not appear to heal more quickly. If further increased, the only expected result would be a smaller temperature gradient through the upper ocean layer.
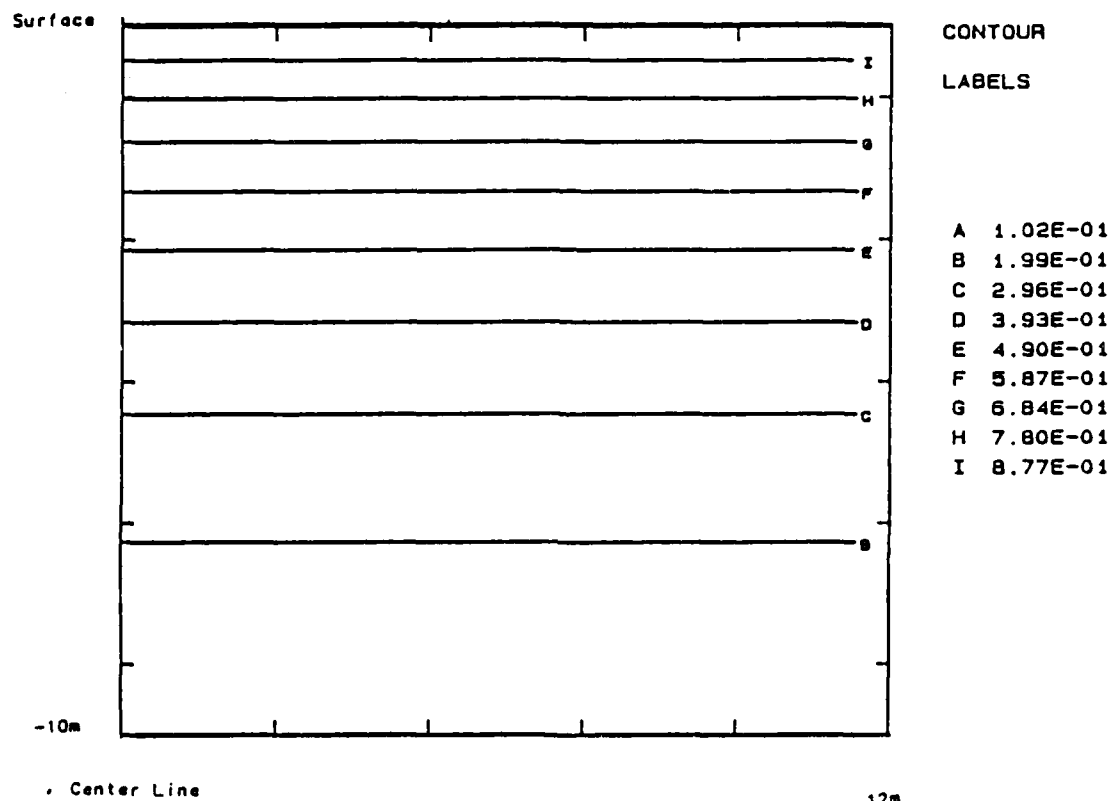
8

Surface

CONTOUR

LABELS

A	1.02E-01
B	1.99E-01
C	2.96E-01
D	3.93E-01
E	4.90E-01
F	5.87E-01
G	6.84E-01
H	7.80E-01
I	8.77E-01

-10m

, Center Line

12m
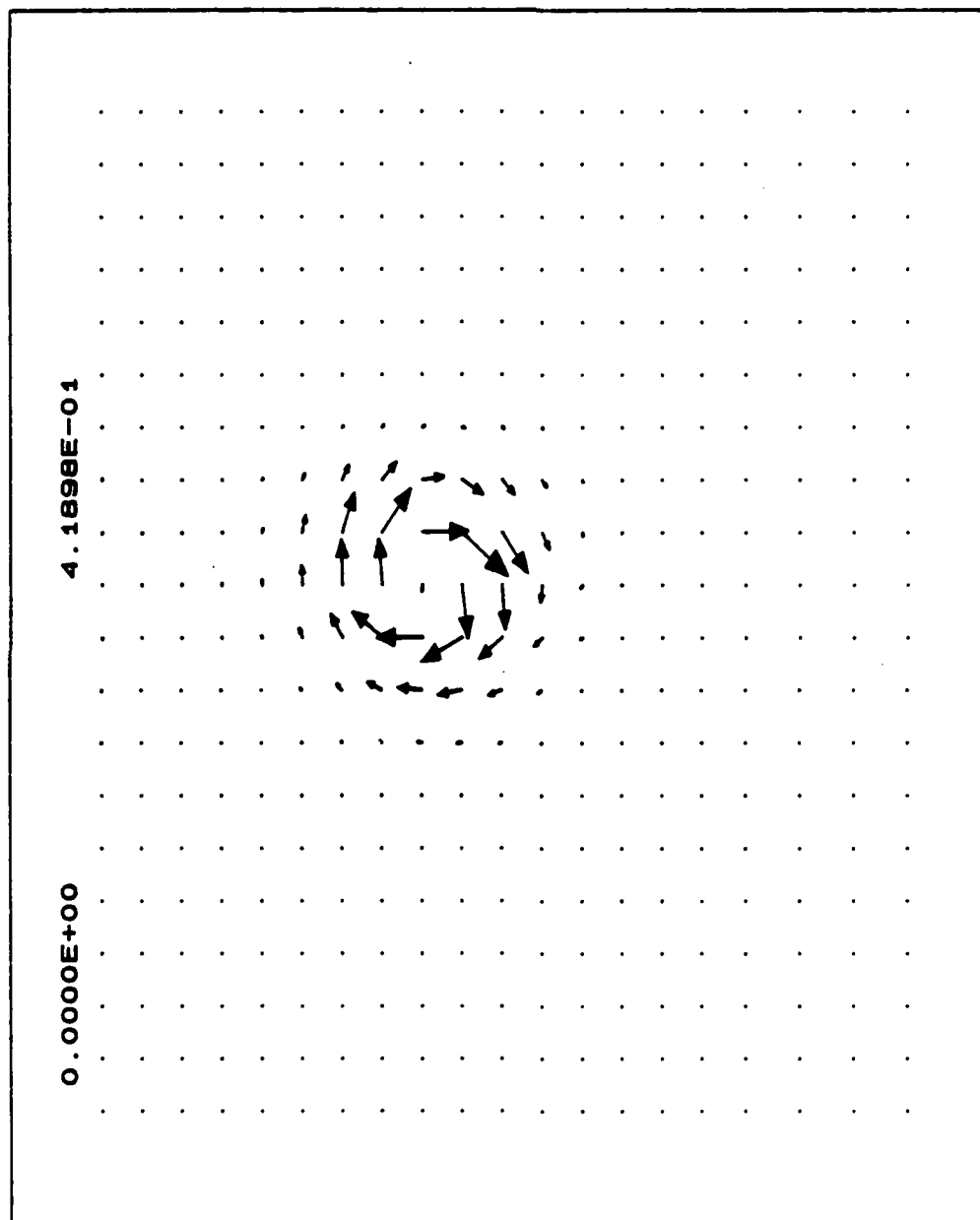
Fig. 2a — Initial Plane Temperatures

9

Fig. 2b — Initial Plane Swirl Velocity

10
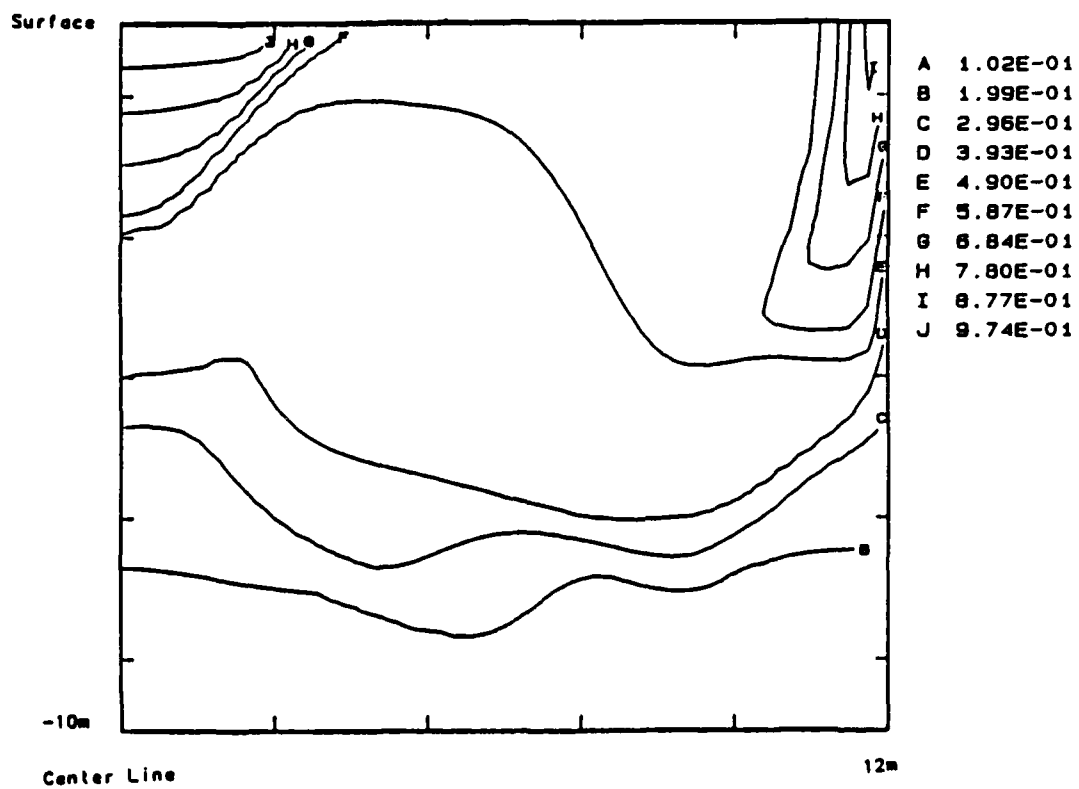
Fig. 3a — Isotherms of Developing Wake, 3 Km

11

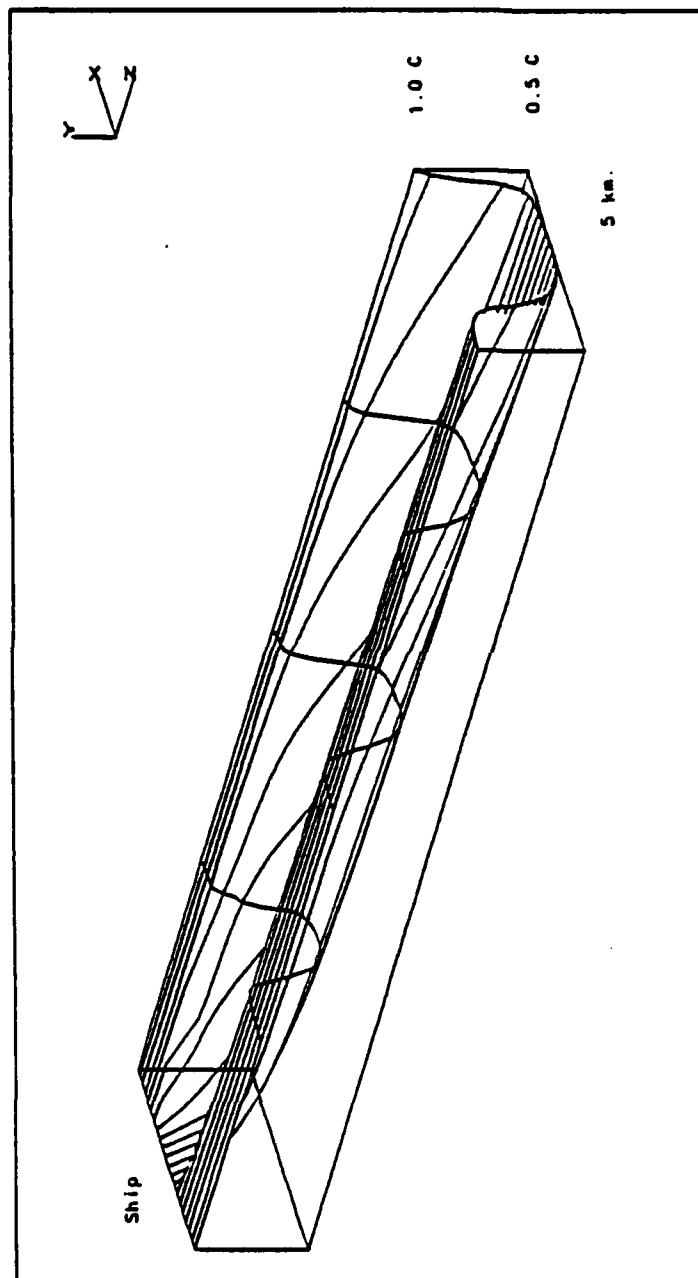Fig. 3b — Surface Temperature of the Developing Wake
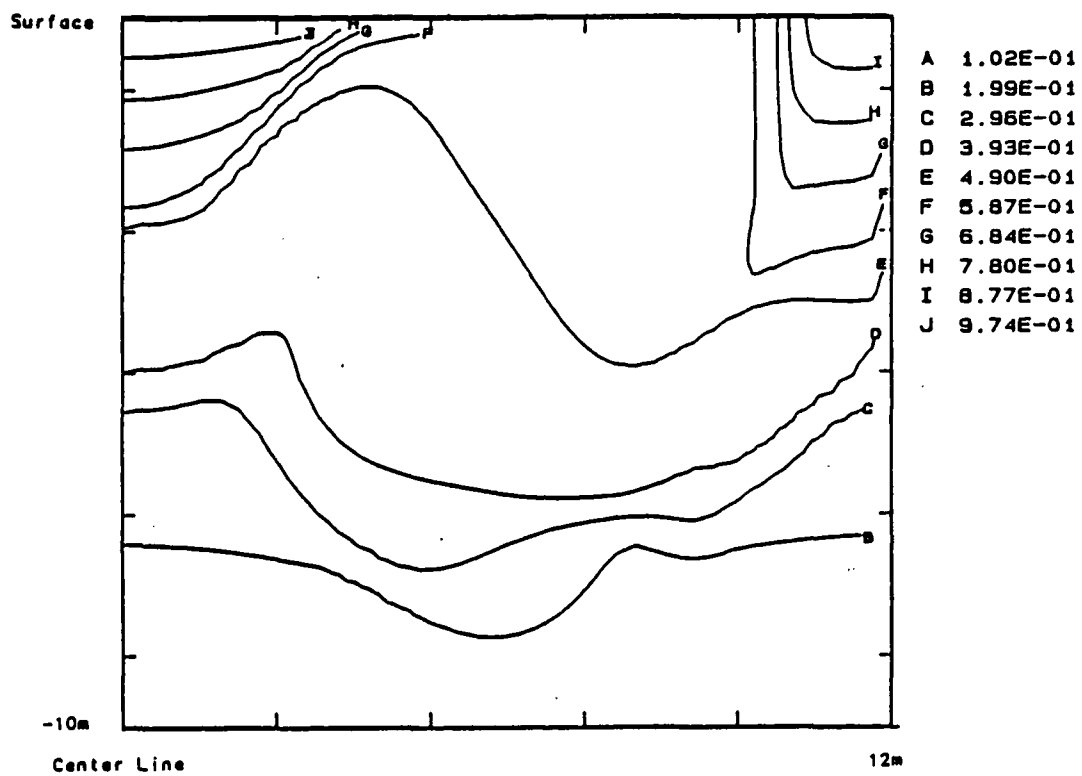
Surface

A	1.02E-01
B	1.99E-01
C	2.96E-01
D	3.93E-01
E	4.90E-01
F	5.87E-01
G	6.84E-01
H	7.80E-01
I	8.77E-01
J	9.74E-01

-10m

Center Line   12m
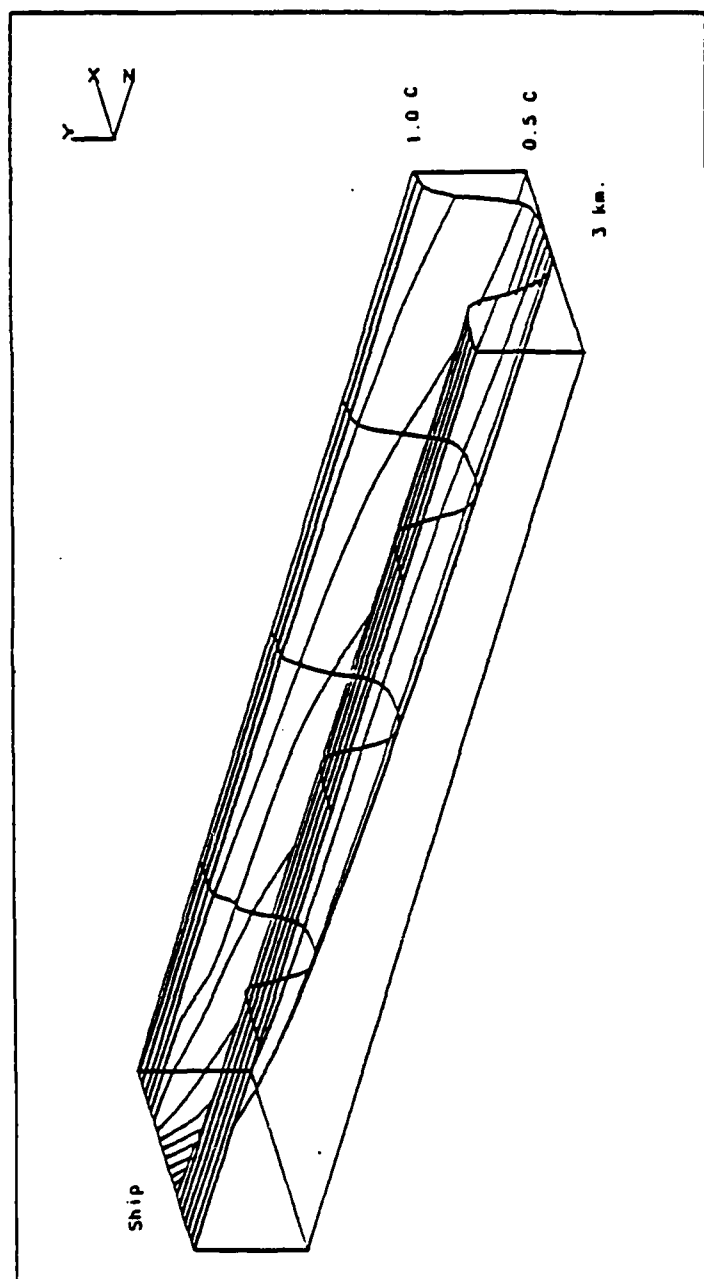
Fig. 4a — High Diffusivity Isotherms

Fig. 4b — High Thermal Diffusivity Surface Temperature

The second mechanism investigated was the effect of anisotropy in the thermal diffusivity caused by horizontal shear layers. This approach is promising because preferential heat transfer in the horizontal direction would cause the surface scar to heal more quickly. Unfortunately, it is also expected to cause the sub-surface wake to heal. This is not in agreement with the limited experimental observations. The results of a two order of magnitude difference in the horizontal and vertical thermal diffusivity are shown in Figs. 5a and 5b. Even this magnitude anisotropy causes only a small effect which is indeed uniform throughout the layer.

Another potential mechanism is the effect of perpendicular wind shear. The component of wind stress perpendicular to the ship track will eventually entrain warm water from areas of the undisturbed ocean upwind of the wake and cover the surface of the thermal scar leaving the sub-surface less disturbed. While this explanation appears inviting, it would only be a factor when a significant component of the wind is perpendicular to the ship track.

This effect is difficult to simulate numerically because perpendicular wind stress violates the symmetry condition used at the wake centerline. It also provides an inflow boundary condition on one edge of the computational domain without specifying a velocity profile. This is not important at an outflow boundary because information is being convected out of the computational area unlike the inflow boundary where information is being convected into the domain.

This situation was modeled by removing the zero normal flow boundary condition on both the vertical transverse plane boundaries and substituting a zero normal velocity gradient condition instead. The alternative was to extend the computational domain to both halves of the wake and far enough from the wake so that a logarithmic velocity profile characteristic of drift currents could be imposed at the inflow boundary. A computational area of this size was unreasonable. The effect of this approximation is to consider only the turbulent shear forces transmitted vertically from the wind stress at the surface and ignore the momentum convected from the established drift current. In cases where the drift current is either very deep or very shallow compared to the wake, this will be a good assumption.

Figures 6a and 6b show the predicted effect of perpendicular wind stress on the thermal wake. Immediately after the ship the wake appears and begins to develop as with the standard wake. The wind stress begins to cover the wake with undisturbed surface water at about 2 km. The scar completely heals between 3 to 5 km downstream. The combined effect of the swirl and establishing drift current on the isotherms is seen in Fig. 6b. All predictions are qualitatively in good agreement with both sets of open ocean measurements (1, 3). One set of informal observations made at the David Taylor Naval Ship Research and Development Center (NSRDC) towing tank did indicate that the wake there healed eventually without the assistance of wind. There are other differences which preclude any conclusions based on this observation. The ambient turbulence levels were not representative, the Reynolds number effects are very different, and the finite width of the towing channel itself could be a factor. Futher experiments there could prove very useful in validating the approaches taken here.

15

Surface

A 1.02E-01
B 1.99E-01
C 2.96E-01
D 3.93E-01
E 4.90E-01
F 5.87E-01
G 6.84E-01
H 7.80E-01
I 8.77E-01
J 9.74E-01

-10m

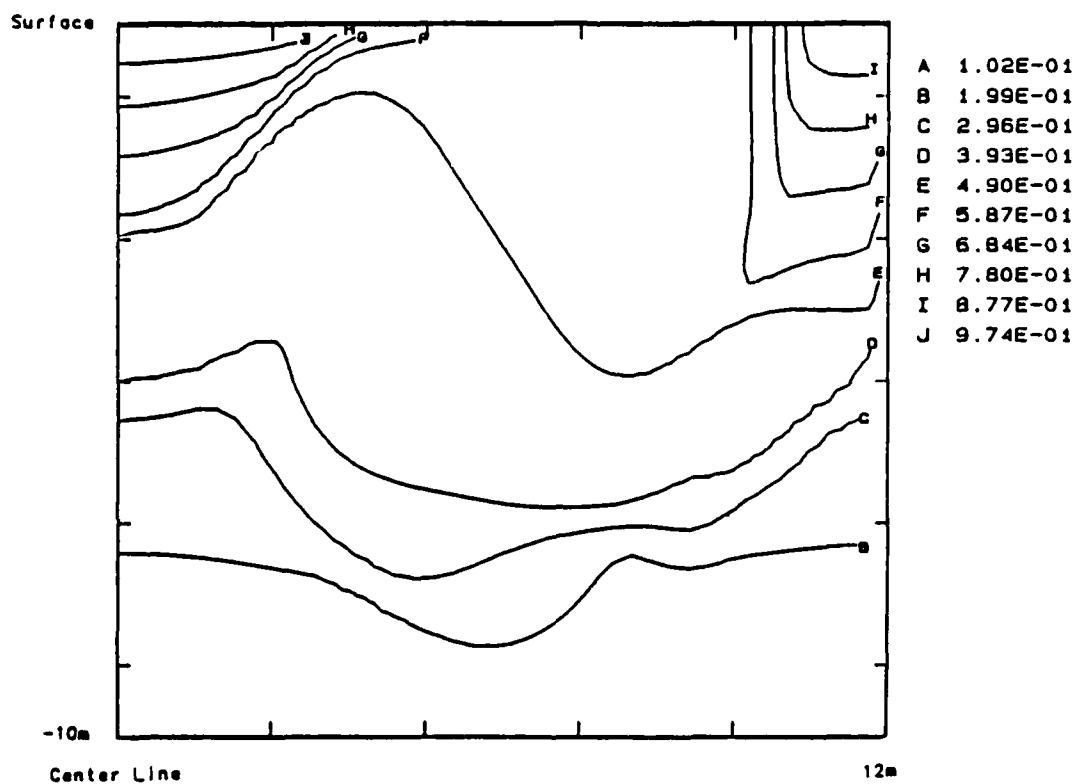Center Line   12m

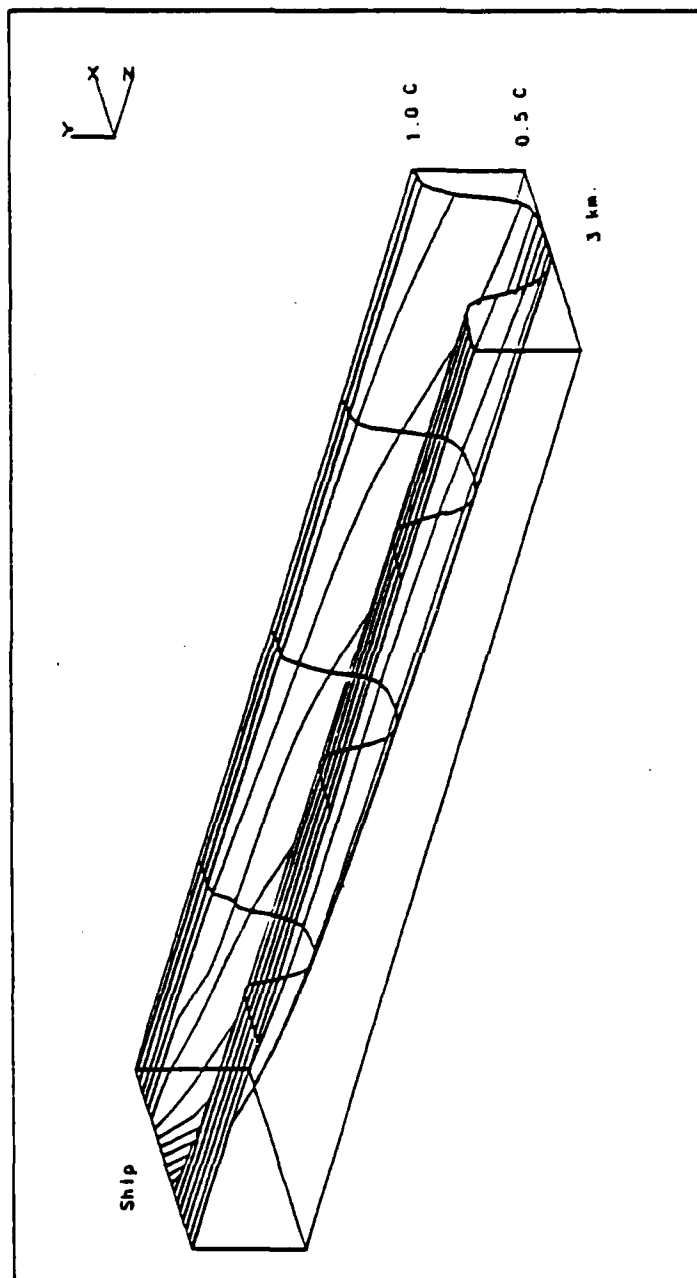Fig. 5a — Anisotropic Thermal Diffusivity Isotherms

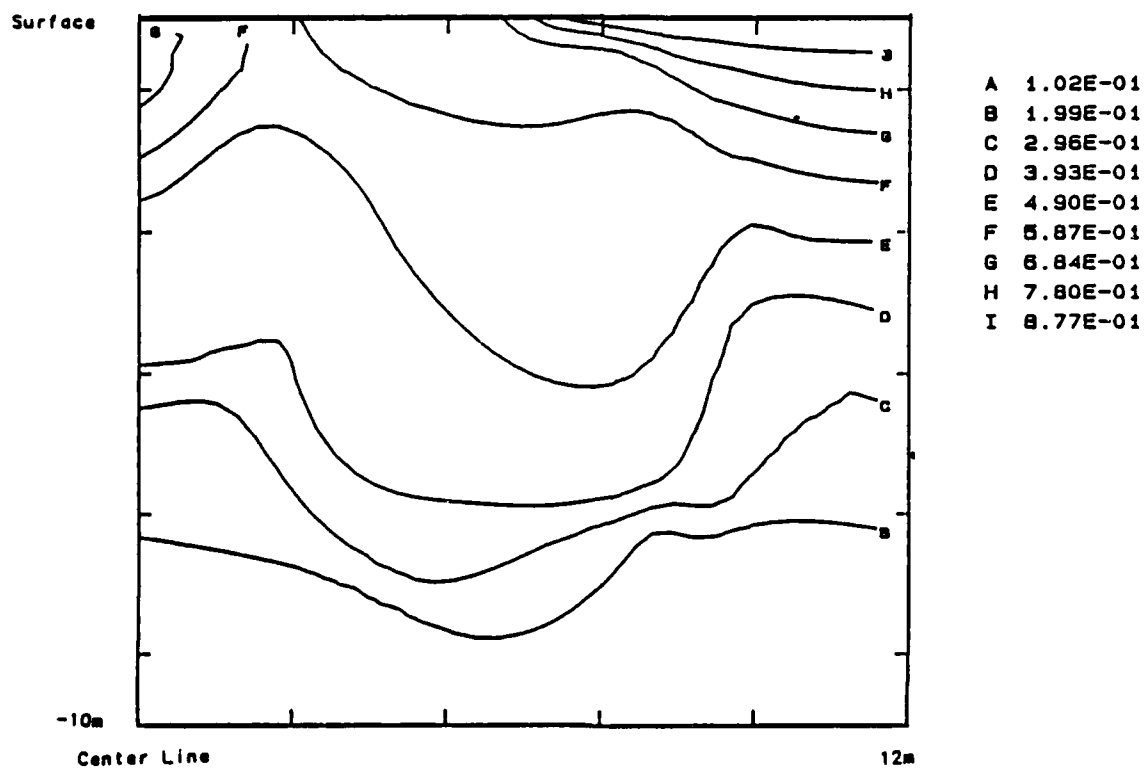Fig. 5b — Anisotropic Thermal Diffusivity Surface Temperature
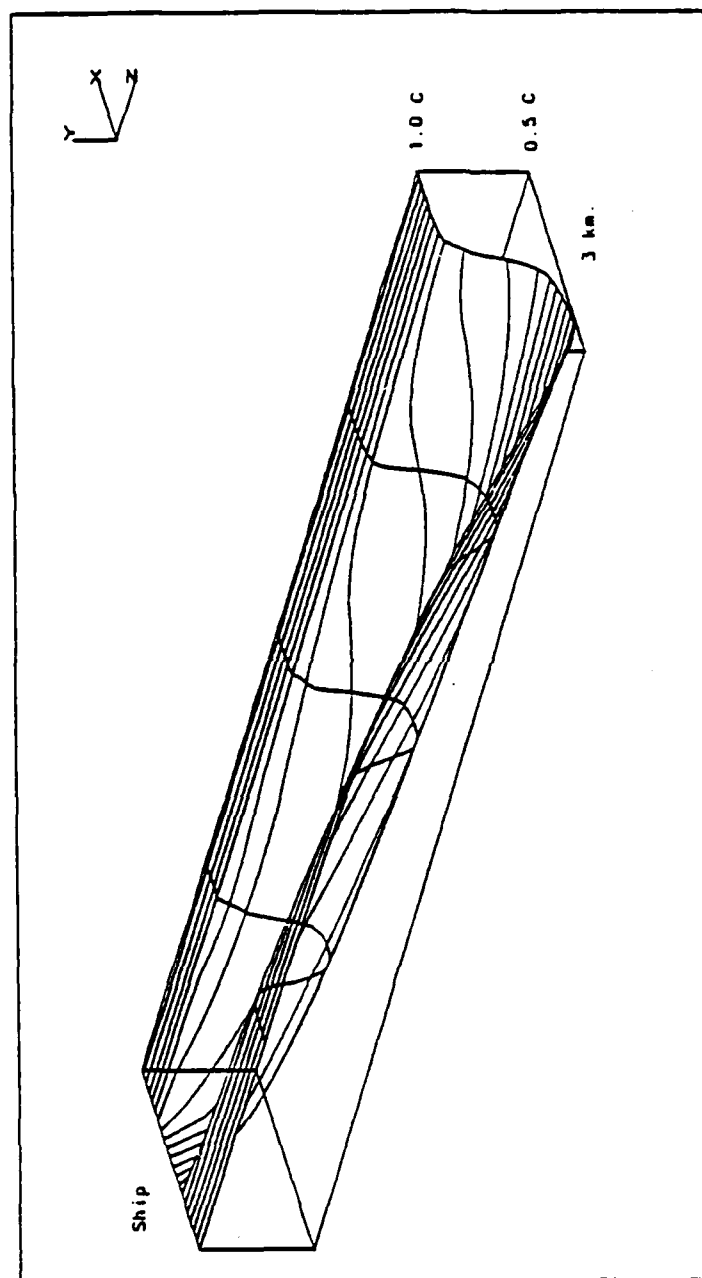
Fig. 6a — Isotherms with Wind Stress

Fig. 6b — Surface Temperature with Wind Stress

Buoyancy Effects

Based on observations made at NSRDC, a mechanism not related to currents or wind drift can, in some instances, cause the thermal wake to disappear. These observations were made in water which probably has low levels of ambient turbulence and measurements taken of the thermal stratification indicate relatively low levels of natural convection. Because all forms of ambient mixing appear to be small, a flow induced mechanism was identified. The buoyancy forces acting on the displaced fluid could provide such a mechanism. In some cases, density variations in the horizontal direction can cause a trailing vortex to break up (16).

The proper form of the buoyancy source term for the vertical component of velocity in a stratified fluid is slightly modified from that found in a fluid of uniform density.

$$S = density * g * beta * (T - T(inf, z))$$

Thus the reference temperature is not a constant but is a stationary function of vertical location (17). This form of the buoyancy force has been used only in semi-confined flows (18). The flow pattern under consideration here is complicated by the imbedded vortex which can become unstable under certain conditions (19).

Simulations using the initial conditions shown in Figs. 2a and 2b indicated that the vortex was destroyed very early in the calculation. There was little of the deformation of the isotherms which were predicted earlier and which have been observed. The kinetic energy of the transverse velocities were quickly converted to potential energy by the small displacement of the stable density stratification.

It appears that this initial temperature distribution is too crude to account for the effects of buoyancy. A first order estimate of the effect of buoyancy requires a well-mixed vortex core temperature which can then rotate without working against the stable density stratification. In this case the effect of buoyancy is confined to the fluid entrained by the vortex. The magnitude of the effect of buoyancy will depend on the size of the well mixed (isothermal) vortex core; a larger isothermal core will be less affected. Unfortunately, there is essentially no information on the initial temperature distributions in the early wakes of ships. An arbitrary core size was chosen such that the core was well mixed where the swirl velocity was .1 m/s or greater.

The results of this calculation are shown in Figs. 7a and 7b. The surface temperature plot shows a reduced signature compared to the standard wake. The isotherms at 5 km show that the effect of the vortex has been reduced. The vortex broke down early in the calculation. Energy is converted from kinetic rotational energy to potential buoyant energy. This is in addition to the effect the entire vortex structure rising or descending due to buoyant forces.

The healing mechanism is seen starting at the end of the computation. Warm water is being drawn over the scar. Even after the primary scar is covered, a less well defined, wider scar will remain. Predictions based on this calculation qualitatively fit the available ocean measurements (3). Quantitative comparisons are not possible because of the differences between the ships used.

Night Wake

A ship moving through the night ocean produces a completely different wake than during the day. Without the solar heating, the largest source of heat transfer is removed. Ambient turbulent mixing quickly eliminates the temperature profile in the upper ocean. Heat transfer to the air occurs only in the top few microns of water primarily through re-radiation to the night sky, latent heat lost by evaporation, and convective heat transfer with the air. The relative importance of each of these terms depends on the atmospheric and ocean conditions. Usually a cooled layer forms on the top of the ocean. Such a cool layer is unstable except at the interface between the water and air where turbulent
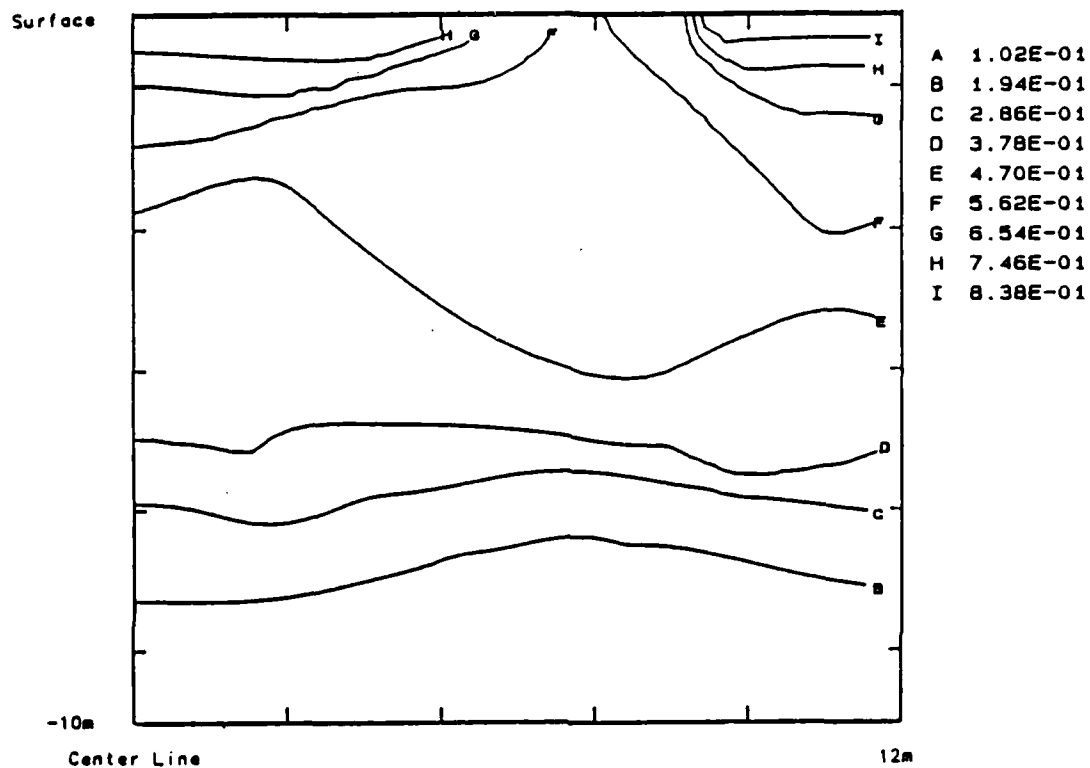
20

Surface

A	1.02E-01
B	1.94E-01
C	2.86E-01
D	3.78E-01
E	4.70E-01
F	5.62E-01
G	6.54E-01
H	7.46E-01
I	8.38E-01

-10m

Center Line   12m

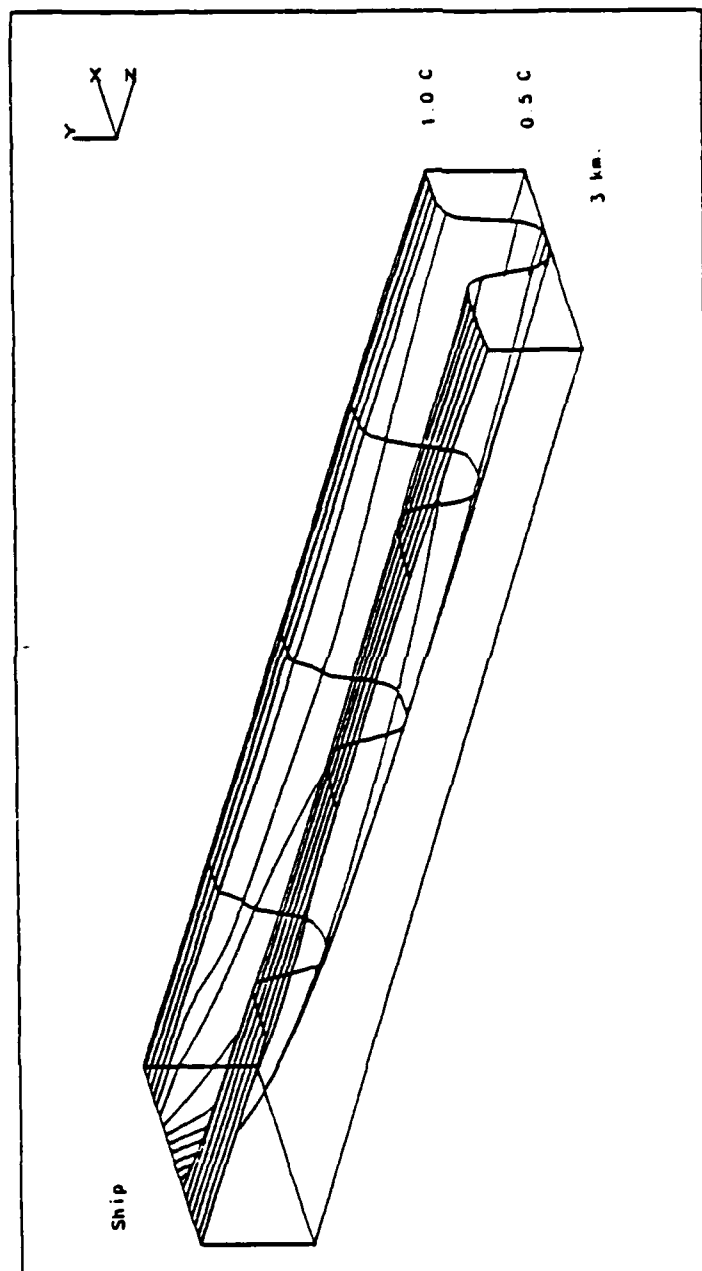Fig. 7a — Isotherms with Buoyancy

21

Fig. 7b — Surface Temperature with Buoyancy

22

fluctuations are damped and a viscous/conductive region forms. As the cool layer tries to grow beyond this layer Rayleigh type instabilities reduce the layer to the viscous thickness.

This layer has been observed in the laboratory and open ocean (13,20). It remains intact through a variety of weather conditions and apparently breaks down only at the onset of wave breaking or a similar vigorous surface disturbance such as a ship passage.

This wake was modeled here by reducing the surface control volumes to the observed thickness of the viscous layer. A vortex will pump water to the surface causing the viscous layer to thin until it reaches the temperature of the subsurface water. The effect will be a warm wake on a cold surface. The thermal scar would heal when the vortex weakened enough to permit heat transfer to the air to again dominate the thinning effect. Because the water is at uniform temperature except at the top node, the energy equation is solved only for the surface nodes.

Figure 8 shows the predicted form of the thermal wake. It appears to be reasonable when compared to the rare (and undocumented) observations (21). Laboratory studies (13) indicate that this mechanism (dilution) is not the cause of the extended wake. The only known mechanism capable of causing the disruption of the cold layer is the surface breaking (breaking waves, the passage of a ship). When these mechanisms cease, the wake re-establishes within 20 seconds. Obviously, the thinning of the layer alone is insufficient to explain the observations of the night wake phenomenon.

Two possible mechanisms which are currently being investigated involve the special biological/chemical characteristics of the surface microlayer (e.g. see ref. 20) and the disruptive behavior of the bubble wake on the sea surface. The biological and chemical surfactants can accumulate on the surface of the sea due to the ship induced vortex and the motion of the bubble wake. Surfactants accumulate preferentially on the air/water interface which makes bubbles particularly effective of concentrating surfactants. Once on the sea surface, the surfactants would disrupt the surface micrlayer until natural diffusion processes could disperse the slick. ᶠ bbles can also distrupt the surface microlayer mechanically by rising to the surface and bursting.

Summary and Conclusions

The numerical model developed here represents a fully parabolic description of the turbulent wake with anisotropic Reynolds stress closure and isotropic turbulent energy closure. Predictions indicate that the initial thermal wake development is in reasonable agreement with the limited observations. The mechanisms which cause the eventual healing of the surface scar while the subsurface thermal disturbance persists were investigated using numerical experimentation.

The most promising physical mechanisms for the observed wake behavior are the effect of perpendicular wind stress and buoyancy. Wind stress appears to be a good candidate for thermal wake healing whenever a significant component of the wind is normal to the wake. The effect of buoyancy was difficult to predict quantitatively because of vortex breakdown which appears to occur early in the wake development. Again, this result is preliminary because good data for comparison are not currently available.

The night wake was predicted assuming that surface spreading caused the breakdown in the viscous cold layer. Although this assumption is debatable, the predictions appeared reasonable compared to limited and qualitative descriptions of the phenomenon.

For both day and night wakes, good quantitative experimental data of the surface and subsurface thermal wake is necessary to verify these predictions or to provide a basis for further model development. In addition, a more basic understanding of vortex propagation in a stratified fluid is required to establish a relationship between buoyancy and vortex breakdown. Finally, the basic dynamics of cold
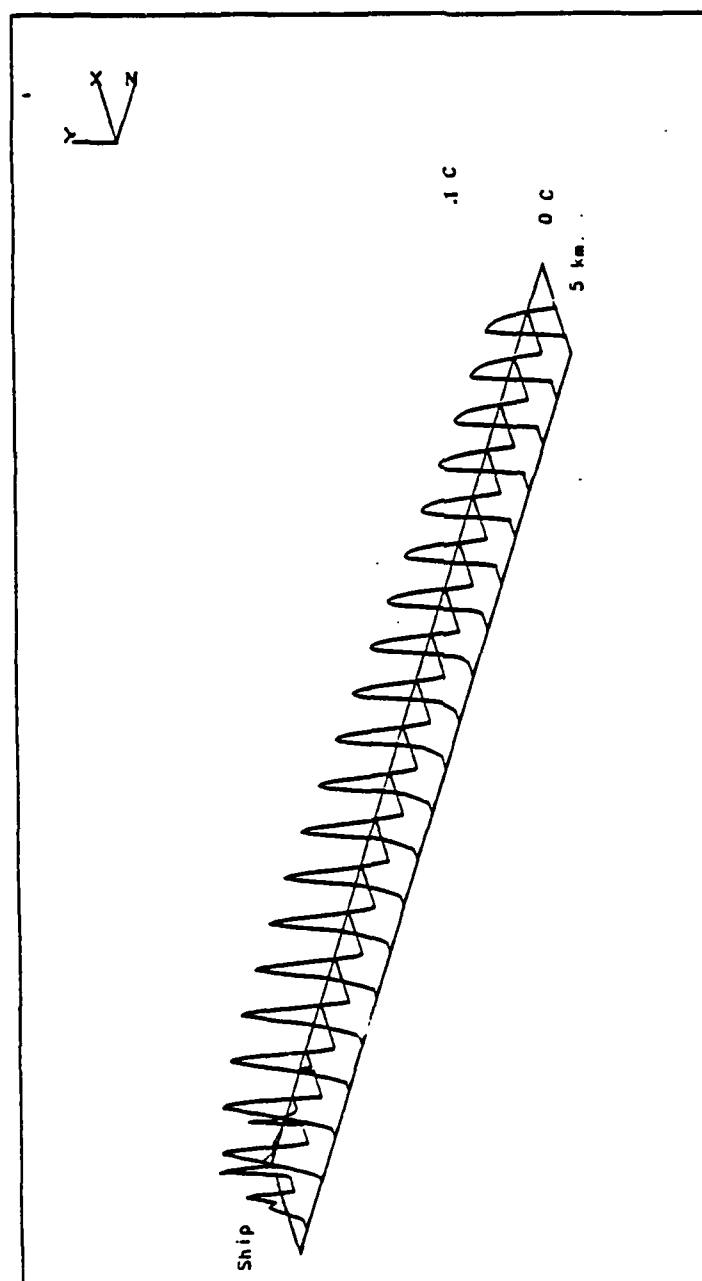
Fig. 8 — Night Thermal Wake

surface layer breakdown and re-formation is also needed for guidance in developing more complete physical models of the night wakes of ships. In view of the scaling difficulties and other limitations associated with laboratory experiments it may be necessary to pursue experiments at or near full scale under carefully selected and documented conditions.

Acknowledgments

References

1. Garber, K.H., Urik, R.J., and Cryden, J. , 1945, "Thermal Wake Detection", USNR&S Laboratory Report, S-20, San Diego

2. Peltzer, R.D., 1984, "White-Water Wake Characteristics of Surface Vessels", NRL Memo Report 5335, Washington, D.C.

3. Peltzer, R.D., 1984, "Remote Sensing of the USNS Hayes Wake", NRL Memo Report 5430, Washington, D.C.

4. Wang, H.T., and Keramidas, G.A., 1986, "Kelvin: An Interactive Computer Code for Kelvin Spectrum with Viscous Correction", NRL Memo Report 5826, Washington, D.C.

5. Lugt, H.J., 1981, "Numerical Modeling of Vortex Flows in Ship Hydrodynamics- a Review", Third International Conference on Numerical Ship Hydrodynamics, Paris

6. Miner, E.W., Griffin, O.M., and Skop, R.A., 1986, "Near-Surface Bubble Motions in Sea Water", NRL Memo Report 5756, Washington, D.C.

7. Smith, R.W., Hyman, M.C., Uzes, C.A., "Convective-Diffusive Bubble Transport in Ship Wakes", NCSC, to be published

8. Garrett, W.D., and Smith, P.M., 1984, "Physical and Chemical Factors Affecting the Thermal IR Imagery of Ship Wakes", NRL Memo Report 5376, Washington, D.C.

9. Swean, T.F.,Jr., Personal Communication, NRL

10. Patankar, S.V., and Spaulding, D.B., 1972, "A Calculation Procedure for Heat, Mass, and Momentum Transfer in Three Dimensional Parabolic Flows", Int. J. of Heat and Mass Trans., Vol. 15, Pergamon Press

11. Baker, A.J., 1982, "The CMC-3DPNS Computer Program for Prediction of Three Dimensional, Subsonic, Turbulent Aerodynamic Juncture Region Flow", NASA Contractor Report 3645, Washington, D.C.

12. Rodi, W., 1980, "Turbulence Models and Their Applications in Hydraulics- A State of the Art Review", IAHR-Section on Fundamentals of Division II: Experimental and Mathematical Fluid Dynamics

13. Hill, R.H., 1977, "Oceanic Thermal Boundary Layer Observations", NRL Memo Report 3538, Washington, D.C.

14. Neumann, G., and Pierson, W.J., Jr., 1966, "Principles of Physical Oceanography", Prentice-Hall, Englewood Cliffs

15. Kamenkovich, V.M., 1977, "Fundamentals of Ocean Dynamics", Elsevier Sci. Pub. Co., Amsterdam

16. Sarpkaya, T. and Johnson, S.K., 1982, "Trailing Vortices in Stratified Fluids", NPS-69-82-003, Naval Post Graduate School, Monterey, Cal.

17. Jaluria, Y., 1980, "Natural Convection Heat and Mass Transfer", Pergamon Press, Oxford

18. Jaluria, Y., 1983, "Buoyancy-Induced Two Dimensional Vertical Flows in a Thermally Stratified Environment", Computers in Fluids, Vol. 11, no. 1, Pergamon Press, Oxford

19. Erickson, G.E., 1981, "Vortex Flow Correlation", AFWAL-TR-80-3143, AFWAL, Wright-Patterson AFB, Ohio

20. Khundzhua, G.G., Gusev, A.M., Andreyev, Y.G., Gurov, V.V., Skorokhvatov, N.A., 1977, "Structure of the Cold Surface Film of the Ocean and Heat Transfer between the Ocean and the Atmosphere," Izvestiya, Atmospheric and Oceanic Physics, Vol. 13, No. 7

21. Hill, R.H., 1986, Personal Communication